Journal of Macromolecular Science, Part A
Publication details, including instructions for authors and subscription information:
http://www.informaworld.com/smpp/title~content=t713597274

Study on Associative Polymerizable Inverse Microemulsion

Hongsheng Lu[ab]; Yujun Feng[a]
[a] Chengdu Institute of Organic Chemistry, Chinese Academy of Sciences, Chengdu, Sichuan, P. R. China [b] Graduate University of the Chinese Academy of Sciences, Beijing, P. R. China

Online publication date: 04 January 2011

To cite this Article Lu, Hongsheng and Feng, Yujun(2008) 'Study on Associative Polymerizable Inverse Microemulsion', Journal of Macromolecular Science, Part A, 45: 5, 372 — 380
To link to this Article: DOI: 10.1080/10601320801946298
URL: http://dx.doi.org/10.1080/10601320801946298

Journal of Macromolecular Science®, Part A: Pure and Applied Chemistry (2008) **45**, 372–380

ISSN: 1060-1325 print/1520-5738 online
DOI: 10.1080/10601320801946298

Study on Associative Polymerizable Inverse Microemulsion

HONGSHENG LU[1,2] and YUJUN FENG[1]

[1]*Chengdu Institute of Organic Chemistry, Chinese Academy of Sciences, Chengdu, Sichuan, P. R. China*
[2]*Graduate University of the Chinese Academy of Sciences, Beijing, P. R. China*

Received September, 2007, Accepted October, 2007

In an effort to determine the suitable polymerizable inverse microemulsion region in pseudoternary phase diagram (PPD), the pseudoternary system of Span80-Tween80/isopar M/aqueous solution of acrylamide and 2-(methacryloyloxyl) ethyl hexadecyl dimethyl ammonium bromide (DM16) was investigated at 40°C. The PPD was obtained by a combination method of turbidimetry and conductivity (CMTC). The reliability of the PPD line was checked by investigating the state of selected experimental points near the boundary line using the Pulsed Near Infrared Light Scattering (PNILS) and centrifugation. Based on the achieved PPD, a series of hydrophobically associating polyacrylamide (HAPAM) microlatex were successfully prepared by choosing the right formulation. It shows that CMTC could be used as a good method in ascertaining a polymerizable inverse microemulsion region, from which optimized HAPAM can be prepared. The factors governing the area of the polymerizable inverse microemulsion region were also discussed.

Keywords: hydrophobically associating polyacrylamide; inverse microemulsion polymerization; pseudoternary phase diagram (PPD); CMTC

1 Introduction

Over the past decades, hydrophobically associating water-soluble polymers (HAWSP) have stimulated increasing attention due to their noticeable ability in controlling the viscosity at various shear rates. Among these polymers, hydrophobically associating polyacrylamide (HAPAM) derived by incorporating a relatively small amount (generally less than 2 mol%) of hydrophobic groups onto a polyacrylamide backbone are especially attractive (1–4). Owing to its excellent viscosity building capacity, this type of polymers has resulted in a wide application in oilfield exploitations, including drilling, polymer- flooding, chemical flooding and profile modification, etc (5–13).

Up to date, the methods for preparing HAPAM by copolymerization could generally be categorized into two routes: micelle polymerization (14–17) and inverse emulsion polymerization (18). However, there are some obvious disadvantages for these methods. The solid content of the resultant polymer by micelle polymerization is relatively low because of the very high viscosity of the final system (19–21), and it is well known that obtained polymers are characterized by blocky distribution of the hydrophobes, compositional inhomogeneity and strong dependence of solution properties on block length (13). The instability of the HAPAM emulsions represents the significant drawback of inverse emulsion process, which results in inconvenience of storage.

Today, a new trend is to adopt the inverse microemulsion polymerization (IMP) techniques to prepare HAPAM. This technique was firstly reported by Candau, et al. in 1982 (22). In their work, polyacrylamide of high molecular weight ($\sim 3 \times 10^6$) was obtained in inverse microemulsions without any additional cosurfactant. This kind of inverse microlatex was stable and transparent; the rate of polymerization was rapid (about half an hour) and the water-solubility of polymer was improved. But the potential of IMP in synthesizing HAPAM was not recognized until 1999, when Candau et al. (23) successfully synthesized HAPAM with a nonionic hydrophobic monomer. These polymers exhibit interesting rheological properties in aqueous solution, such as shear-shinning, shear-thickening, viscoelasticity and so on (24). As could be seen from their work, IMP could be regarded as an effective tool in synthesizing HAPAM. Unfortunately, such promising technology has not yet provoked extensive attention in synthesizing HAPAM, and up to now, only a a small number of literature on both theoretical and practical research have been reported (23, 24).

Address correspondence to: Hongsheng Lu, Chengdu Institute of Organic Chemistry, Chinese Academy of Sciences, No. 9, Section 4, Renmin South Road, Chengdu, Sichuan 610041, P. R. China; E-mail: phdhshlu@yahoo.com.cn or Yujun Feng, Chengdu Institute of Organic Chemistry, Chinese Academy of Sciences, No. 9, Section 4, Renmin South Road, Chengdu, Sichuan 610041, P. R. China. Tel.: +86 28 85236874; Fax: +86 28 85236874; E-mail: yjfeng@cioc.ac.cn

Currently, our attention is focused on obtaining further insight on the theory of HAPAM polymerizable inverse microemulsion systems. It has come to be realized that the success of IMP of HAPAM is, to a large extent, hampered by the complex formulation of the reaction system. Therefore, the question remains on how to obtain a reliable phase diagram region, in which all the formulations could prove to be adoptable. In the present work, an attempt was made to determine the suitable reaction condition for IMP of acrylamide with cationic hydrophobic monomer. This should be based on the obtainment of a reliable PPD. To the best of our knowledge, this was the first systematic investigation on the polymerizable inverse microemulsion containing a cationic hydrophobic monomer. Such information could not only provide further insight of inverse microemulsion systems for preparing HAPAM, but also could be used as guidance for future industrial processes.

2 Experimental

2.1 Materials

Acrylamide (AM), produced via a biocatalytic process, was purchased from Changjiu Agri-Scientific Chemicals Co., Ltd. (Jiangxi, China). It was recrystallized twice with chloroform (m.p. 84°C) and stored in silica gel desiccators prior to use. Isopar M, an isoparaffinic mixture with a boiling temperature range of 223–254°C, was purchased from Exxon Mobile (TX, USA). Span80 (HLB = 4.3) and Tween80 (HLB = 15.0) were obtained from Kelong Reagent Co. Ltd. (Chengdu, China). Other reagents were all of analytical grade. Water (resistivity $> 18\ M\Omega\ cm^{-1}$) was prepared by distillation three times. 2-(methacryloyloxyl) ethylhexadecyldimethylammonium bromide (DM16, Figure 1) was synthesized in our lab (see Section 2.2). 2,2′-azobis(2-methylpropionamidine) dihydrochloride (V50) (97 wt.%, Aldrich) was used as received.

2.2 Synthesis of DM16

A 500 mL flask was charged by a certain amount of acetone, n-hexadecyl bromide and 2-(dimethylamino) ethyl methacrylate (the molar ratio was 1:1). The flask was placed at room temperature for 48 h. The crude production was purified by filtration, followed by washing with the mixture solvent of acetone and ethyl acetate (3:1 v/v) three times before it was dried under a vacuum oven at 25°C for 48 h. Finally, the final product, DM16 with a white powder appearance, was obtained.

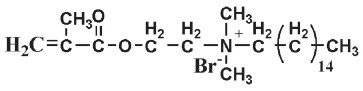

Fig. 1. The molecular structure of DM16.

2.3 Determination of PPD

The value of HLB could be calculated with the well-known Griffin Equation (25):

$$\mathrm{HLB} = \frac{(W_A \times \mathrm{HLB}_A + W_B \times \mathrm{HLB}_B)}{(W_A + W_B)} \quad (1)$$

where W_A, W_B, HLB_A, and HLB_B are the mass of A and B, the HLB of A and B, respectively. It is necessary to point out that the usable range is confined to the nonionic surfactant.

A 250 mL thermostatic, double-walled glass container with a circulation of water was charged by a certain amount of mixture of Isopar M, Span80 and Tween80. Then the aqueous solution dissolving acrylamide, DM16 and resorcinol (used as inhibitor in order to prevent the monomers from polymerization) was slowly added to the mixture comprising of surfactants and Isopar M in an intermittent manner. The emulsification was conducted at 40°C (except special illustrations, all work was carried out at this temperature) under vigorous stirring (at a speed of about 1000 rpm). The dropping of aqueous solution was terminated when the optically transparent inverse microemulsion turned into the turbid inverse emulsion. Generally, the transition point for an experimental point was achieved by keeping the system for 2 days, and the time required was obviously shorter than what was reported elsewhere (26).

It should be pointed out that, during the whole process, the dropping rate and amount of aqueous solution should be strictly controlled according to the value changes of conductivity of the microemulsion. The values of conductivity for any two adjacent experimental points should be very small. This could no doubt effectively enhance the success probability and reduce experimental errors. The conductivity was measured with a DDS-11A conductometer (Fangzhou Instrument, Chengdu) in conjunction with platinum electrodes embedded in glass (cell constant $= 1.04\ cm^{-1}$, provided by the manufacturer). Sufficient time was allowed between successive additions (every 5 min) for the system to reach equilibrium (22).

2.4 Reliability Analysis of CMTC

2.4.1 Pulsed Near Infrared Light Scattering

The stability and transparency were measured by a pulsed near-infrared light scattering spectrometer (Turbiscan MA2000). The sample to be analyzed is contained in a cylindrical glass measurement cell. The reading head, Turbihead, is composed of a pulsed near-infrared light source ($\lambda = 850$ nm) and two synchronous detectors. The transmission detector receives the light which goes through the sample (0°), while the backscattering detector receives the light backscattered by the sample (135°). Turbihead scans the entire length of the sample (about 65 mm), acquiring transmission and backscattering data every 40 μm.

Thus, we obtain transmission and backscattering profiles, i.e., curves giving the transmitted and backscattered light flux (%, relative to external standards) as a function of the

sample height (mm). These profiles constitute the macroscopic fingerprint of the sample at a given time. In a schematic way, we can obtain an important transmission signal (and a very small one in backscattering) when dispersions are transparent to turbid, and it is the contrary for opaque dispersions. The measurement is conducted at 40 ± 0.1°C.

2.4.2 Centrifugation

The centrifugation technique has recently been applied to the study of microemulsions which provides information on the nature and the stability of the continuous phase (27) Centrifugation experiments were performed with a B800 centrifuger (Sukun Instrument, Shanghai, China) for the surfactant/oil/aqueous solution systems so as to measure the stability of the mixture system and to check the reliability of the PPD boundary line. The measurements were conducted at 40 ± 0.1°C.

Three different systems were analyzed with the centrifuges. The ra-11 located at the right side of boundary line, ra-12 and ra-13 located at the left side of boundary line. All the selected points were set very near to the PPD boundary line. Their compositions were listed in Table 1.

2.5 Applicability of Microlatex Preparation by PPD

2.5.1 Microemulsion Polymerization

A 250 mL three-neck flask fitting with a mechanical stirrer was charged by a certain amount of Isopar M, Span80 and Tween80. The temperature was kept constant at 40°C. The aqueous solution containing acrylamide and DM16 was added dropwise within 20 min. The speed of stirring was 1000 rpm and the stirring time was 4 h. Then, purified nitrogen was bubbled in the microemulsion for 45 min to eliminate oxygen. Finally, the initiator (V50) solution was injected under stirring (300 rpm) and the reaction time was 4 h. The beginning stage of the polymerization was evidenced by a change from the transparency of the microemulsion to a slightly bluish coloration. The polymerization was rapid and an almost total conversion of monomers was achieved. The final system could remain clear and stable over months. Their viscosity was very low, usually within the range of a few centipoises.

2.5.2 Characterization of Microemulsion

Particle diameters were determined by a laser light scattering spectrometer (BI200SM) equipped with a digital correlator (BI9000AT). The scattered light from an Argon laser (514.5 nm) was used for measurement at 90°. The translational diffusion coefficient D and the hydrodynamic radius R_h were obtained from the average decay rate Γand Stokes–Einestein equation as shown below:

$$D = \frac{\Gamma}{q^2} \tag{2}$$

$$R_h = \frac{kT}{6\pi\eta D} \tag{3}$$

Here, the scattering vector q could be calculated from Equation (4):

$$\mathrm{q} = \frac{4\pi \mathrm{n}}{\lambda \sin(2\theta)} \tag{4}$$

where θ, λ, k, T, η, and n are the scattering angle, the incident wavelength in vacuum, the Boltzmann constant, temperature, solvent viscosity and solvent refractive index, respectively. The size of inverse microemulsion before polymerization was measured directly. All the samples were prepared by filtering of 1 ml of the microlatex solution with a 0.45-μm Millipore filter into a clean scintillation vial. The microlatex was diluted with Isopar M down to a volume fraction of the dispersed phase of around 0.5–5% (28).

Table 1. Sample compositions to prove the reliability of boundary line

No.	Isopar M (wt.%)	Surfactant (wt.%)	Aqueous solution (wt.%)	HLB
ra-11	51.83	27.91	20.26	9.2
ra-12	28.11	42.16	29.73	9.2
ra-13	80.15	14.15	5.69	9.2

3 Results and Discussion

In general, an effective way to obtain microemulsion is to induce the transition of emulsion-microemulsion by increasing the surfactant concentration. The transition is usually sharp and could be detected turbidimetrically, visually or conductively. The line connected by all of transition points is called boundary line in the PPD. In this work, the transition points were determined with the maximal weight fraction of aqueous phase (A_{max}) under the given ratio of surfactant to oil.

Generally, a single method to obtain phase transition point presents some disadvantages, such as difficulty in precisely controlling the transition points, considerable time and labor consumption, and relatively greater errors. In order to overcome these shortcomings, an effective means is to combine two or more methods together. For convenience of discussion below, we term our method as Combinative Methods of Turbidimetry and Conductivity (CMTC) to determine PPD.

3.1 Reproducibility of the Experiment

The parallel experiments were performed. As shown in Figure 2, the resultant curves indicated the boundary of inverse emulsion (left) and inverse microemulsion (right) domains. It could be seen that the two resultant curves obtained by CMTC were superposed, which suggested that the method to obtain PPD exhibits good reproducibility. So, it is suitable for the obtainment of a pseudoternary phase diagram.

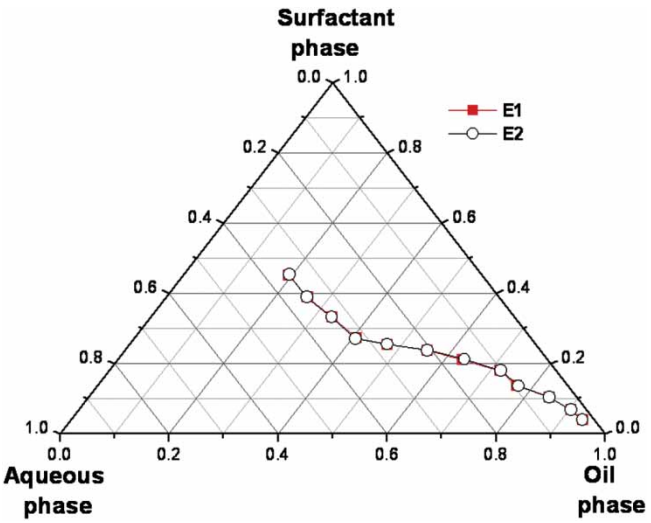

Fig. 2. The reproducibility of pseudoternary phase diagram obtained by CMTC. The systems consisted of a monomers aqueous solution (aqueous phase, 53.9%), Isopar M (oil phase) and Span80-Tween80 mixture (surfactant phase). The molar ratio of AM to DM16 was 99:1. The value of HLB is 9.2.

3.2 Validation of the Reliability of PPD

In order to check the reliability of the PPD boundary line obtained by CMTC, three coordinate points near the boundary line were selected. First, the PPD boundary line was thought to be reliable, i.e., the inverse emulsion region located at the left side of boundary line and the inverse microemulsion region located at the right side of the boundary line. It means that ra-11 could form transparent stable inverse microemulsion; ra-12 and ra-13 could only form opaque unstable inverse emulsion when the phase balance was reached. Secondly, the stability and transparency of ra-11, ra-12 and ra-13 were measured when the phase balance was reached. If all the measured results did completely tally with the postulation, the PPD boundary line could be considered reliable, whereas it is unreliable. Their compositions were listed in Table 1.

As shown in Figure 3, the transmission of the system (ra-11) was about 80% (high transparency). During scanning in 2 h, the scanning lines (back scattering) were nearly confined to a narrow band, indicating the stability of the analytes (the typical character of inverse microemulsion: stable, transparent). The transmission of the system (ra-12) is about zero (ra-12 is milk-white after emulsification). The scanning lines were dispersed and spacious, illustrating that this system was unstable (the typical character of inverse emulsion: unstable, turbid). Likewise, although the system (ra-13) exhibits a certain degree of transmission, the transmission lines and back scattering lines became more and more loose and spacious with the time lapse, suggesting the instability of the analytes (the typical character of inverse emulsion). The stability of this analyte deteriorates during the entire scanning process.

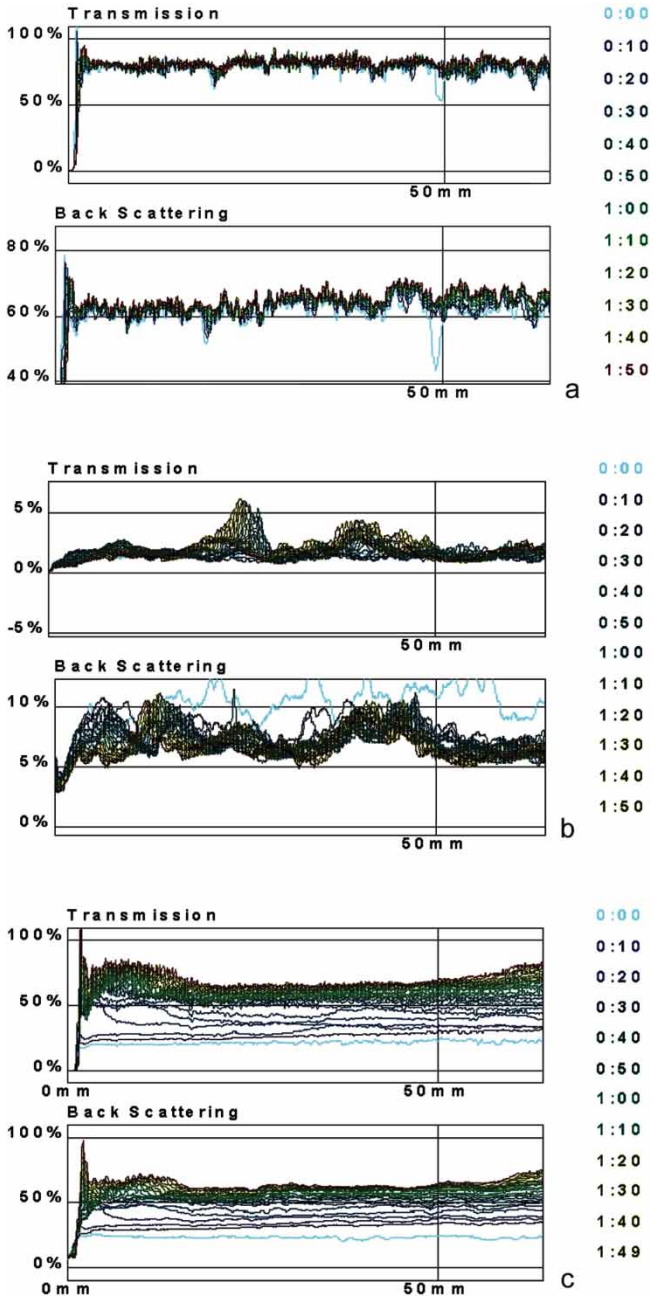

Fig. 3. The results of pulse near infrared light scattering (ra-11: a; ra-12: b; ra-13: c) (the abscissa is the entire length of the sample, the right y-axis is the time of scanning).

In the same way, the three sample systems after emulsification were centrifuged with 8000 rpm for 60 min. The photographs (Figure 4) were taken before and after centrifugation. After centrifugation, ra-11 was still transparent and stable, but an obvious phase separation was observed for both for ra-12 (the upper was transparent and the lower appear white cream like) and ra-13 (the upper was transparent and the lower appeared as a yellow oil), indicating the instability of ra-12 and ra-13.

From the above discussions, the experimental data or phenomena proved what had been postulated. It illustrated

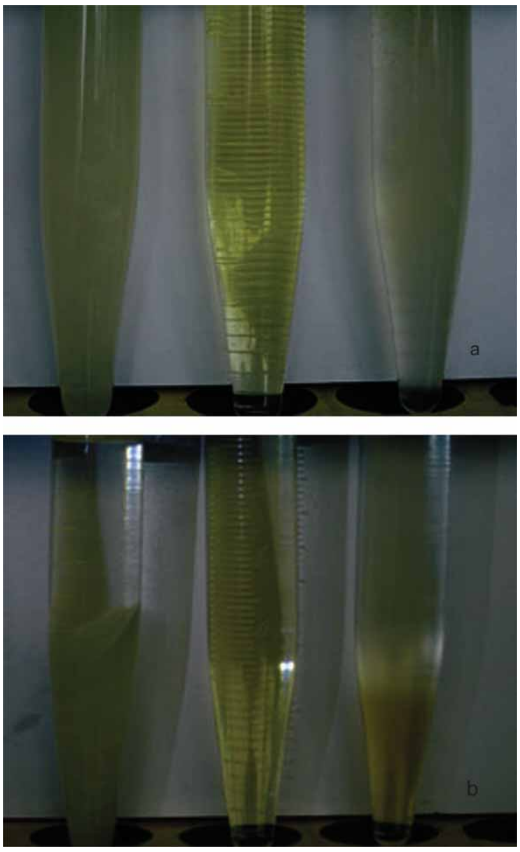

Fig. 4. Photographs of the samples before centrifugation (a) and after centrifugation (b): ra-11 (middle), ra-12 (left) and ra-13 (right).

the reliability of the PPD boundary line. This could in turn prove the correctness of the methods (CMTC) used throughout the experiment.

3.3 Validation of the Feasibility

Based on the PPD, a series of HAPAM microlatex (the formulation was in an inverse microemulsion region) was successfully prepared. On the contrary, the formulation (in the inverse emulsion region, i.e., A11 and A13) could not prepare microlatex but a milk-white emulsion-latex or layered latex. The characteristics of the systems were given in Table 2.

After polymerization, the microlatex was stable and transparent. Using a laser pen to irradiate the microlatex, a slick beam of light could be observed, which exhibited a strong Tyndall effect. However, due to the larger size of the particles and the higher refractive index of the HAPAM compared with the monomer, the latexes dispersed more light than the initial microemulsions. It was in good agreement with literature (29).

As noted in Table 2, the diameter of inverse microemulsion was measured before and after polymerization. Before polymerization, the diameter is about 3 nm, which is similar with ordinary microemulsion. But after polymerization, the diameter of microlatex varies from 65 to 118 nm. Furthermore, there is no settlement and turbidity for any system located at the right side of the PPD boundary line before polymerization and after polymerization. As shown in Figure 5, the polymerization was rapid and an almost total conversion of monomers was achieved. It is in good agreement with the report elsewhere (27, 31–35). All these proved the feasibility of selecting suitable conditions to prepare HAPAM according to PPD.

3.4 Effect of HLB on PPD

The first step in HAPAM synthesis with inverse microemulsion polymerization was the determination of the compositions forming the stable inverse microemulsion. A comparison was made among the PPDs in the presence of monomers (AM and DM16) in the aqueous phase. As could be seen in Figure 6, these systems corresponded to large volume fractions of the disperse phase and consequently to high monomer concentrations. For a lower mass ratio of surfactants to oil, the area of the inverse microemulsion region was almost independent of HLB. However, when the mass ratio of surfactant to oil was larger than 0.123, the case was quite different. One could understand it in this way, only the optimal matching of the chemical structure for the oil and the mixture surfactant could result in the existence of the maximal A_{max}, but the A_{max} may have tiny differences under a low surfactant weight fraction. By comparison, HLB = 8.8 exhibited the maximal area of the inverse microemulsion region. All these HLB needed to form inverse microemulsion were

Table 2. Summary of the polymerization system

							Size (nm)			Appearance	
No.	HLB	Isopar M (g)	Surfactant (g)	AM (g)	DM16 (g)	Water (g)	Initial (g)	Initial system	Final system	Initial system	Final system
A25	9.2	80	40	11.64	0.72	10.78	0.015	3	118	Clear	Clear stable
A27	9.2	80	40	11.64	0.72	10.78	0.070	3	65	Clear	Clear stable
A29	9.2	80	40	11.64	0.72	10.78	0.05	3	89	Clear	Clear
A11	9.2	80	10	11.64	0.72	10.78	0.05	/	/	Milk white	White latex
A13	9.2	80	15	11.64	0.72	10.78	0.05	/	/	Milk white	Layered

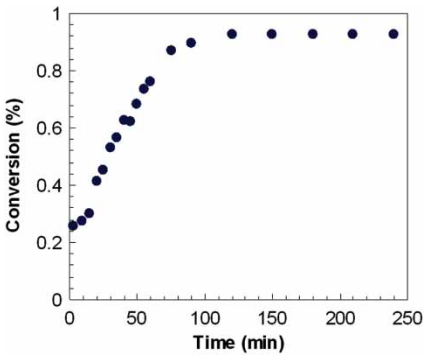

Fig. 5. The monomer conversion plotted as a function of time for sample A29.

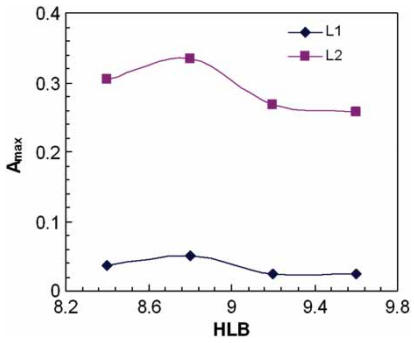

Fig. 7. Maximal weight fraction of aqueous phase (A_{max}) vs. the HLB for microemulsion-emulsion transition with a given mass ratio of surfactant to oil: (L1) 0.123 and (L2) 1.

bigger than that described by the classical microemulsion theory explained by Candau (22, 23).

As indicated in Figure 7, the curves exhibited a maximum (A_{max}) for an optimum HLB value, which is close to 8.8 for most of the mass ratio of surfactant to oil. This effect was likely to be associated with a good matching of the chemical structure for the oil and the surfactant when the number of HLB was 8.8. Furthermore, both AM and DM16 might as well locate at the water/oil interface, which made the interfacial layer become more closely packed, functioning as a stabilizing factor (31). As a result, the following will focus on discussion at HLB = 8.8.

3.5 Effect of Monomers' Concentration on PPD

Another attention-getting question is the optimization of the concentration of aqueous phase and monomers to obtain stable HAPAM microlatex with a maximum microlatex concentration. As shown in Figure 8, the area of the inverse microemulsion region was relatively great. These curves all exhibited a turning point. Therein, the turning point may give prominence to the role of cosurfactant of AM (36). At a low mass ratio of surfactant to oil (namely, under the turning point), all the A_{max} was small, bearing almost a linear relation. The area was almost independent of the monomers' concentration. Above the turning point, the A_{max} depended on the monomers' concentration, resulting in the relatively serious difference of the area of the inverse microemulsion region. It is obvious that there is the minimal area of inverse microemulsion when the monomers' concentration is 50.0%. This is more obviously reflected in Figure 9, i.e., the minimal A_{max} appears at HLB = 8.0.

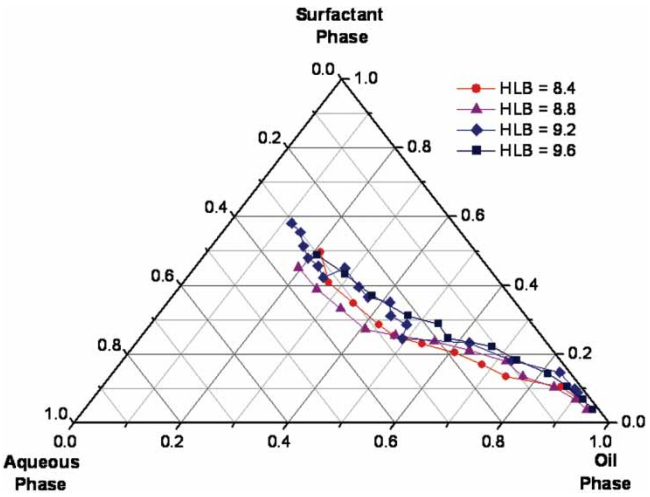

Fig. 6. Influence of HLB. The systems consisted of a monomers aqueous solution (aqueous phase, 53.9%), Isopar M (oil phase) and Span80-Tween80 mixture (surfactant phase). The molar ratio of AM to DM16 was 99:1.The resultant curves indicated the boundary of inverse emulsion (left) and inverse microemulsion (right) domains.

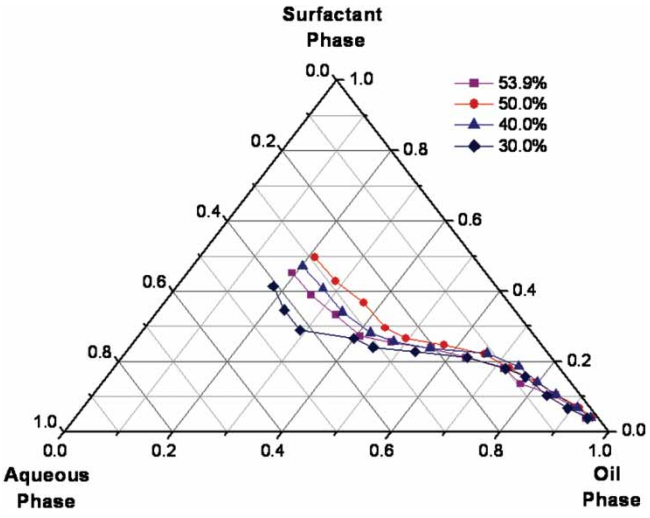

Fig. 8. Influence of monomers' concentration (C_m) in aqueous solution. The systems consisted of a monomers aqueous solution (aqueous phase, different monomer concentrations), Isopar M (oil phase) and Span80-Tween80 (surfactant phase, HLB = 8.8). The molar ratio of AM to DM16 was 99:1.The line was the boundary line between the inverse emulsion (left) and inverse microemulsion (right) domains.

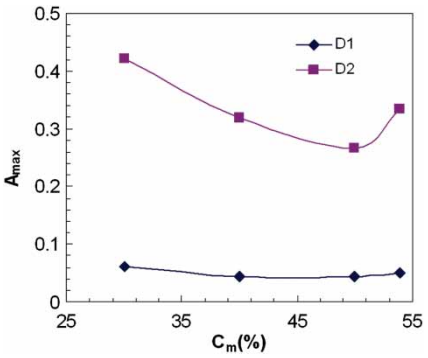

Fig. 9. Maximal weight fraction of aqueous phase (A_{max}) vs. the monomers' concentration (C_m) in aqueous solution for microemulsion-emulsion transition with a given mass ratio of oil and surfactant: (M1) 0.123 and (M2) 1.

Although AM could also be seen as a cosurfactant (22, 23), the increase of the AM concentration could not absolutely extend the area of polymerizable inverse microemulsion region more and more with the monomers' concentration (27). It could be ascribed to the existence of the optimal matching of cosurfactant and surfactant on the interface between oil and water.

Fortunately, as reflected in Figure 10, no matter how the mass ratio of surfactant to oil, the monomers' weight fraction in the whole inverse microemulsion system increased with the concentration of monomers. Therefore, the high solid content HAPAM microlatex could be obtained at a high concentration of monomers in aqueous solution. Figure 10 also indicated that when the concentration of monomers in aqueous solution reached 53.9%, the inverse microemulsion system possessed a relatively high M_{max}. This value was smaller than what reported elsewhere (37), which could result from the difference of hydrophobic monomers and surfactant.

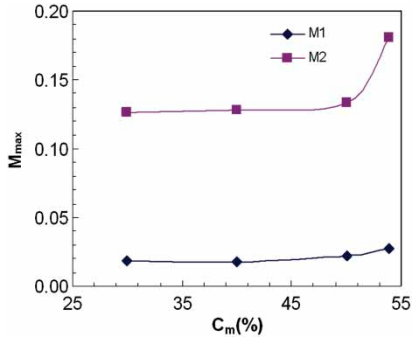

Fig. 10. Maximal weight fraction of monomers (M_{max}) vs. the monomers' concentration (C_m) in aqueous phase for microemulsion-emulsion transition with given mass ratio of oil and surfactant: (M1) 0.123 and (M2) 1.

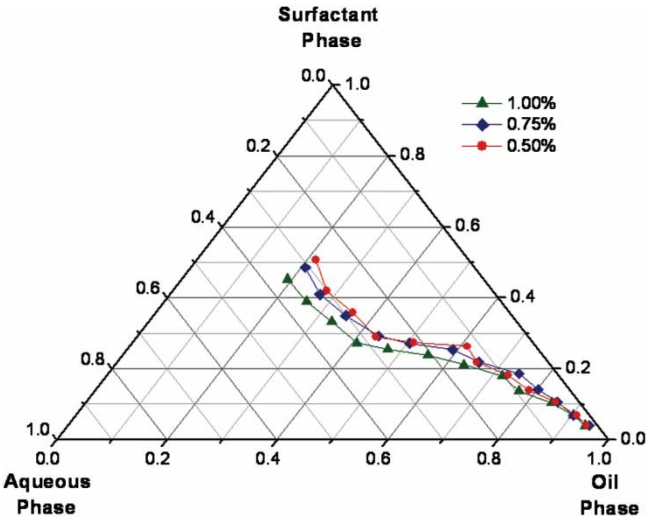

Fig. 11. Influence of the molar fraction of DM16. The systems consisted of a monomers aqueous solution (aqueous phase, 53.9%), Isopar M (oil phase) and Span80-Tween80 (surfactant phase, HLB = 8.8). The molar ratio of AM to DM16 varied from 99:1 to 99.5:0.5. The line is the boundary line between the inverse emulsion (left) and inverse microemulsion (right) domains.

3.6 Effect of Monomers Feed Ratio on PPD

As indicated in Figure 11, the area of the inverse microemulsion region increased with the ratio of DM16 to AM. Under low ratio of surfactant to oil, the molar ratio of DM16 to AM had no notable influence in the area of inverse microemulsion region. But for a high ratio of surfactant to oil, it was the other way around. Since DM16 is a special surfactant instead of a cosurfactant, the hydrocarbon chain could locate at the interface directly and then be distributed in the oil. In other words, it might make the interfacial layer condensed (stabilizing interface) or loose (breaking interface) (32, 34). However, whether DM16 takes part in emulsification directly or helps to emulsify was not clear. No related literature reported similar phenomena. It could be speculated that there is good matching of the solubility parameters for DM16 and

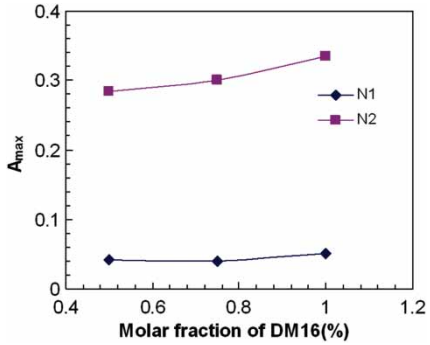

Fig. 12. Maximal weight fraction of aqueous phase (A_{max}) vs. the molar fraction of DM16 for microemulsion-emulsion transition with given mass ratio of oil and surfactant: (N1) 0.123 and (N2) 1.

Span80-Tween80, resulting in the increase of the area of the inverse microemulsion region with the increase of the molar ratio of DM16 to AM.

Figure 12 also indicated that whatever the mass ratio of surfactant to oil was, the A_{max} increased with the ratio of DM16 to AM, resulting in the increase of the area of the inverse microemulsion region. It also shows DM16 redounds to the stability of oil-water interface. Combining all experimental phenomena, one could obviously guess the different existence status of AM (in the interfacial layer or in aqueous phase).

4 Conclusions

This paper reported a new method, namely the combinative method of turbidimetry and conductivity (CMTC), to obtain the pseudoternary phase diagram (PPD) of microemulsions. It shows that CMTC was a good method to obtain PPD, with better reproducibility, reliability, and accuracy than previous methods reported elsewhere (23, 38). Moreover, such a method is very convenient, because it is time-and-labor-effective. By using this method, a series of HAPAM microlatex were successfully prepared in our lab, suggesting the feasibility of selecting a proper formulation to prepare HAPAM microlatex. Therefore, it can also be used as guidance for future research in synthesizing HAPAM, especially for the industrial process.

In a following step, the factors in influencing the area of the polymerizable inverse microemulsion region were carefully investigated. The results show that the hydrophobic monomer (DM16) plays an important role in regulating the stability of the polymerizable inverse microemulsion. In the future, more effort should be exerted to study how to increase the content of monomers in the microemulsion system, and further research is in progress.

5 Acknowledgments

Financial supports from the Chinese Academy of Sciences, the Ministry of Science and Technology of China through its "Hi-Tech 973 program" (2005CB221302), Sichuan provincial Fund (05GG-021-028-05), Opening funds from the State Key Laboratory of Polymer Materials Engineering (200604) and State Key Laboratory of Oil/Gas Geology and Exploitation Engineering (PLN0605) are greatly acknowledged.

6 References

1. Bock, J., Valint, P.L., Jr., Pace, S.J., Siano, D.B., Schulz, D.N. and Turner, S.R. *Water-Soluble Polymers for Petroleum Recovery*; Stahl, G.A. and Schulz, D.N. (eds.); Plenum Press: New York, 147–160, 1998.
2. Bock, J., Varadaraj, R., Schulz, D.N. and Maurer, J.J. *Macromolecular Complexes in Chemistry and Biology*; Dubin, P., Bock, J., Davies, R.M., Schulz, D.N. and Ties, C. (eds.); Springer: Berlin Heidelberg: New York, 33, 1994.
3. Glass, J.E. and Karunasena, A. (1989) *Polym. Mater. Sci. Eng.*, **61**, 145–149.
4. Glass, J.E. *Associative Polymers in Aqueous Media*; ACS Symposium Series, Series 765, American Chemical Society: Washington, DC, 2000.
5. Glass, J.E. *Hydrophilic Polymers: Performance with Environmental Acceptability*; Advances in Chemistry, Series 248, American Chemical Society: Washington, DC, 1996
6. Glass, J.E. *Polymers in Aqueous Media: Performance through Association*; Advances in Chemistry, Series 223, American Chemical Society: Washington, DC, 1989
7. Glass, J.E. *Water-Soluble Polymers: Beauty with Performance*; Advances in Chemistry, Series 213, American Chemical Society: Washington, DC, 1986
8. Schulz, D.N. and Bock, J. (1991) *J. Macromol. Sci., Chem. A*, **28**, 1235–1241.
9. Schulz, D.N., Bock, J. and Valint, P.L., Jr. *Macromolecular Complexes in Chemistry and Biology*; Dubin, P., Bock, J., Davies, R.M., Schulz, D.N. and Ties, C. (eds.); Springer: Berlin Heidelberg: New York, Chapter 3, 1994.
10. Shalaby, S.W., McCormick, C.L. and Butler, G.B. *Water-Soluble Polymers: Synthesis, Solution Properties and Applications*; ACS Symposium Series 467, American Chemical Society: Washington, DC, 1991
11. Schulz, D.N. and Glass, J.E. *Polymers as Rheology Modifiers*; ACS Symposium Series 462, American Chemical Society: Washington, DC, 1991
12. Wang, T.K., Iliopoulos, I. and Audibert, R. (1988) *Polym. Bull.*, **20**, 577–582.
13. Candau, F. and Selb, J. (1999) *Adv. Colloid Interface Sci.*, **79**, 149–172.
14. Bastiat, G., Grassl, B. and François, J. (2002) *Polym. Int.*, **51**, 958–965.
15. Bastiat, G., Grassl, B. and François, J. (2005) *J. Colloid Interface Sci.*, **289**, 359–370.
16. Schulz, D.N., Kaladas, J.J., Maurer, J.J. and Bock, J. (1987) *Polymer*, **28**, 2110–2115.
17. Yahaya, G.O., Ahdab, A.A., Ali, S.A., Abu-Sharkh, B.F. and Hamad, E.Z. (2002) *Polymer*, **42**, 3363–3372.
18. Pabon, M., Corpart, J.M., Selb, J. and Candau, F. (2004) *Journ. of Appl. Polym. Sci.*, **91**, 916–924.
19. Feng, Y.J., Billon, L., Grassl, B., Khoukh, A. and Francois, J. (2002) *Polym.*, **43**, 2055–2064.
20. Huang, Z.Y., Lu, H.S. and He, Y. (2006) *Colloid Polym. Sci.*, **285**, 365–370.
21. Taylor, K.C. and Nasr-El-Din, H.A. (1998) *J. Petro. Sci. Eng.*, **21**, 129–139.
22. Leong, Y.S. and Candau, F. (1982) *J. Phys. Chem.*, **86**, 2269–2271.
23. Candau, F., Pabon, M. and Anquetil, J.Y. (1999) *Colloids Surf. A.*, **153**, 47–59.
24. Zhao, Y. and He, B. (2000) *ACTA Polymer Sinica*, **(5)**, 550–554.
25. Griffin, J.R. and Coughanowr, D.R. (1965) *AIChE Journal*, **11**, 133–137.
26. Zhao, H., Wu, Z. and Zheng, X. (2005) *Acta Petrolei Sinica (Petroleum Processing Section)*, **21**, 43–47.
27. Candau, F., Leong, Y.S., Pouyet, G. and Candau, S. (1984) *J. Colloid Interface Sci.*, **101**, 167–183.
28. Zhao, H.Y., Liu, S.Y., Jiang, M., Yuan., X.F., An, Y.L. and Liu, L. (2000) *Polymer*, **41**, 2705–2709.

29. Saenz deBuruaga, A., de la Cal, J.C. and Asua, J.M. (2000) *Polym.*, **41**, 1269–1276.
30. Candau, F., Zekhnini, Z. and Durand, J.P. (1986) *J. Colloid Interface Sci.*, **114**, 398–408.
31. Candau, F., Leong, Y.S. and Fitch, R.M. (1985) *J. Polym. Sci.: Polym. Chem. Ed.*, **23**, 193–214.
32. Holtzscherer, C. and Candau, F. (1988) *J. Colloid Interface Sci.*, **125**, 97–110.
33. Candau, F., Buchert, P. and Krieger, I. (1990) *J. Colloid Interface Sci.*, **140**, 446–473.
34. Barton, J. (1996) *Prog. Polym. Sci.*, **21**, 399–438.
35. Buchert, P. and Candau, F. (1990) *J. Colloid Interface Sci.*, **136**, 527–540.
36. Rentería, M., Mũnoz, M., Ochoa, J.R., Cesteros, L.C. and Katime, I. (2005) *J. Polym. Sci. Polym. Chem.*, **43**, 2495–2503.
37. Li, X. and Yuan, H. (1999) *China Synthetic Rubber Industry*, **22**, 220–224.
38. Zhang, Y., Zheng, X. and Wei, T. (2004) *Acta Petrolei Sinica (Petroleum Processing Section)*, **20**, 40–45.